

Electronic Supplemental Information

Boosting Artificial Nicotinamide Cofactor Systems

Ioannis Zachos,^{†a} Samed Güner,^{*a} Arabella Essert,^{✉a} Peta Lommes^{#a}, Volker Sieber,^{*,⊙a,b,c,d}

a. Chair of Chemistry of Biogenic Resources, Technical University of Munich, Campus Straubing for Biotechnology and Sustainability, Schulgasse 16, 94315 Straubing, Germany

b. Catalysis Research Center, Technical University of Munich, 85748 Garching, Germany

c. SynBioFoundry@TUM, Petersgasse 5, 94315 Straubing, Germany

d. School of Chemistry and Molecular Biosciences, The University of Queensland, 68 Copper Road, St. Lucia, Queensland 4072, Australia

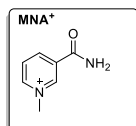
Experimental Section

Materials and methods

All chemicals used in this work were of analytical grade and were purchased from Sigma-Aldrich if not stated otherwise. Enzymes for cloning and site-directed mutagenesis were ordered from New England Biolabs (Germany, Frankfurt). DNaseI and lysozyme were bought from AppliChem GmbH (Germany, Darmstadt) and Carl Roth (Germany, Karlsruhe), respectively. *E. coli* BL21 (DE3) strain from Invitrogen (Germany) was used for overexpression as well as cloning experiments.

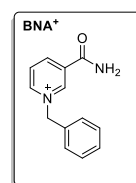
Synthesis of artificial nicotinamide cofactor biomimetics

Synthesis of 3-carbamoyl-1-methylpyridinium chloride (MNA⁺)¹



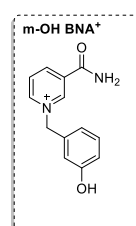
Nicotinamide (50 mmol) was dissolved in 30 mL methanol. Methyl iodide (150 mmol) was added, and the reaction mixture was stirred for 27 h at room temperature. The yellow precipitate was filtered and washed twice with methanol. The crude product was recrystallized from 250 mL hot methanol. C₇H₉N₂O; yellow solid; Yield: 81 %; ¹H NMR (400 MHz, DMSO) δ 9.3 (s, 1H), 9.0 (d, 1H), 8.8 (d, 1H), 8.5 (s, 1H), 8.2 (dd, 1H), 8.1 (s, 1H), 4.4 (s, 3H).

Synthesis of 1-benzyl-3-carbamoylpyridinium chloride (BNA⁺ Cl⁻)



25 g nicotinamide was dissolved in 250 mL acetonitrile at 100 °C in a 500 mL round bottom flask. Subsequently, 26 mL (chloromethyl)benzene was added using a dropping funnel, and the reaction mixture was stirred (750 rpm) under reflux (165 °C) for 65 h. After cooling to room temperature, 50 mL of diethyl ether was added, and the precipitate was filtered and washed twice with diethyl ether. The product was purified using Soxhlet extraction with ethyl acetate. Crystalline powder was dried with a desiccator. White solid; Yield: 85 %.

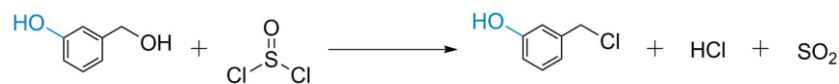
Synthesis of 3-carbamoyl-1-(4-hydroxybenzyl)pyridin-1-ium chloride (meta-OH BNA⁺ Cl⁻)



4 g Hydroxybenzyl alcohol (32 mmol) were dissolved in 80 mL acetonitrile (ACN) and cooled to 4 °C under continuous stirring. 4.2 mL triethylamine (TEA) were added. Afterwards 4.2 mL thionyl chloride (SOCl₂) in 10 mL ACN were slowly added using a dropping funnel. After stirring 1 h at 0 °C reaction was finished. Reaction mixture was concentrated using a rotary evaporator prior to isolation of meta-Hydroxybenzyl chloride using a silica column with ethyl acetate/cyclohexane (10:1) as mobile phase. A purple red powder was obtained after drying in a rotavapor. In a second part 4 g nicotinamide were dissolved in 100 mL ACN at 100 °C. meta-hydroxybenzyl chloride was added using a dropping funnel, and the reaction mixture was stirred (750 rpm) under reflux (165 °C) for 65 h.

After cooling to room temperature, 50 mL of diethyl ether was added, and the precipitate was filtered and washed twice with diethyl ether. The product was purified using Soxhlet extraction with ethyl acetate. Powder was dried with a desiccator. White/yellowish solid; Yield: 20 %. Purity: 85% ¹H NMR (400 MHz, D₂O) δ 9.25 – 9.20 (m, 1H), 8.97 – 8.90 (m, 1H), 8.83 – 8.75 (m, 1H), 8.18 – 8.03 (m, 1H), 7.24 (td, *J* = 7.3, 3.3 Hz, 1H), 6.94 – 6.82 (m, 3H), 5.71 (d, *J* = 2.7 Hz, 2H), 4.66 (d, *J* = 2.7 Hz, 3H), 1.98 – 1.88 (m, 1H).

A



B

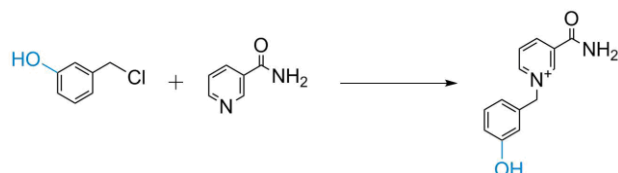
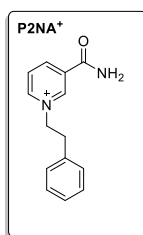


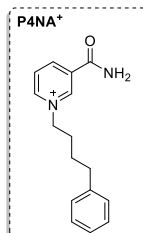
Figure S1 Synthesis route of (A) the precursor 3-(chloromethyl)phenol by chloration of 3-(hydroxymethyl)phenol using thionyl chloride followed by (B) synthesis of meta-hydroxybenzyl nicotinamide (m-OH-BNA⁺ Cl⁻) following an S_N2 reaction of 3-(chloromethyl)phenol and nicotinamide.

Synthesis of 3-carbamoyl-1-phenethylpyridinium chloride (P2NA⁺ Cl⁻)



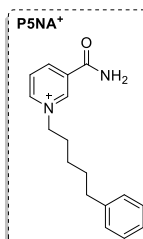
19.67 g nicotinamide (~160 mmol) was dissolved in 180 mL acetonitrile at 105 °C in a 500 mL round bottom flask and heated to reflux. Subsequently, 22 mL (2-chloroethyl) benzene was added using a dropping funnel, and the reaction mixture was stirred under reflux (130 °C) for 150 h. After cooling to room temperature, 50 mL of diethyl ether was added, and the precipitate was filtered and washed twice with diethyl ether. The product was purified using Soxhlet extraction with ethyl acetate. C₁₄H₁₅ClN₂O; white solid; yield: 61 %; ¹H NMR (400 MHz, D₂O) δ 8.9 (s, 1H), 8.7 (d, 1H), 8.6 (d, 1H), 7.9 (d, 1H), 7.2 (m, 3H), 7.0 (m, 2H), 4.8 (t, 2H), 3.2 (t, 2H).

Synthesis of 3-carbamoyl-1-(4-phenylbutyl) pyridinium bromide (P4NA⁺ Br⁻)



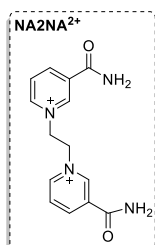
5 g nicotinamide was dissolved in 50 mL acetonitrile at 105 °C in a 250 mL round bottom flask. Subsequently, 5 g (4-bromobutyl)benzene (>97.0%) was added using a dropping funnel, and the reaction mixture was stirred under reflux (130 °C) for 150 h. After cooling to room temperature, 50 mL of diethyl ether was added, and the precipitate was filtered and washed twice with diethyl ether. The product was purified using Soxhlet extraction with ethyl acetate. White solid; yield: 41 %; ¹H NMR (400 MHz, D₂O) δ 9.09 (s, 1H), 8.84 (dtt, 1H), 8.74 (dt, 1H), 8.04 (dd, 1H), 7.15 (m, 5H), 4.55 (t, 2H), 2.56 (t, 2H), 1.94 (m, 2H), 1.57 (m, 2H).

Synthesis of 3-carbamoyl-1-(5-phenylpentyl) pyridinium bromide (P5NA⁺ Br⁻)



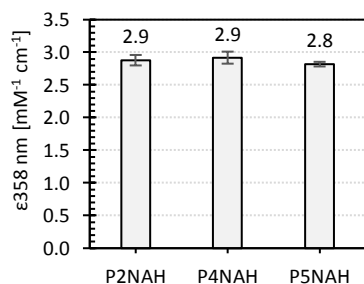
5 g nicotinamide was dissolved in 50 mL acetonitrile at 105 °C in a 250 mL round bottom flask. Subsequently, 5 g (5-bromopentyl)benzene (>98.0%) was added using a dropping funnel, and the reaction mixture was stirred under reflux (130 °C) for 150 h. After cooling to room temperature, 50 mL of diethyl ether was added, and the precipitate was filtered and washed twice with diethyl ether. The product was purified using Soxhlet extraction with ethyl acetate. White solid; yield: 41 %; ¹H NMR (400 MHz, D₂O) δ 9.09 (s, 1H), 8.84 (dtt, 1H), 8.74 (dt, 1H), 8.04 (dd, 1H), 7.15 (m, 5H), 4.55 (t, 2H), 2.56 (t, 2H), 1.94 (m, 2H), 1.57 (m, 2H).

Synthesis of 1,1'-(ethane-1,2-diyl)bis(3-carbamoylpyridin-1-ium) dibromide (NA2NA²⁺ 2Br⁻)



120 mmol nicotinamide (14.65 g) were dissolved in 60 mL CH₃CN in a round bottom flask. Subsequently, 60 mmol 1,2-dibromoethane was added using a dropping funnel, and the reaction mixture was stirred under reflux (130 °C) for 150 h. After Soxhlet extraction NMR showed a product mixture of 80 % final product (NA2NA²⁺) and 20 % of the intermediate (1-(2-bromoethyl)-3-carbamoylpyridin-1-ium). The purified slightly brownish mixture was dissolved together with 4 g nicotinamide in methanol and stirred again under reflux (105 °C) for 24 h. After cooling to room temperature, 50 mL of diethyl ether was added, and the precipitate was filtered and washed twice with diethyl ether. The product was purified using Soxhlet extraction with ethyl acetate. A white precipitation with >99 % purity was achieved. Yield: 20 %. ¹H NMR (400 MHz, D₂O) δ 9.09 (s, 1H), 8.84 (dtt, 1H), 8.74 (dt, 1H), 8.04 (dd, 1H), 7.15 (m, 5H), 4.55 (t, 2H), 2.56 (t, 2H), 1.94 (m, 2H), 1.57 (m, 2H).

In situ reduction of biomimetics for determination of extinction coefficient



To determine the extinction coefficient (ϵ) we reduced different amounts of the cofactor biomimetics P2NA⁺ Cl⁻, P4NA⁺ Br⁻ and P5NA⁺ Br⁻ (0.05 mM – 2 mM) on an MTP Plate (Greiner 96-well, F-bottom) using a 2.5-fold excess of sodium dithionite. Nowak et al. reported 2.9 mM⁻¹ cm⁻¹ for P2NAH that was used to validate the method. All measured biomimetics show similar ϵ of 2.8 - 2.9. Note: Na₂Na²⁺ and its reduced states NAH₂Na⁺ and NAH₂NAH absorb at multiple wavelength (300 nm, 333 nm and 358 nm) which may change over time suggesting stability issues with this cofactor analogue. Calculations for Na₂Na are based on HPLC derived data. m-OH-BNA⁺ was not tested due to the mentioned reasons in the main manuscript.

Molecular biology section

Heterologous production of enzymes

Enzymes were made using auto induction² (AI) medium. Enzymes were produced similar to Nowak et al. 2017.³ In short a single colony of *E. coli* BL21 (DE3) bearing plasmids with a gene of interest was grown over night in 100 mL baffled flask containing 10 mL LB medium supplemented with 100 $\mu\text{g mL}^{-1}$ kanamycin at 37 °C, 150 rpm. In the following day, the 10 mL culture was transferred to a 5 L baffled flask containing 1 L AI medium supplemented with 100 $\mu\text{g}\cdot\text{mL}^{-1}$ kanamycin or carbenicillin. The culture was shaken at 120 rpm. Different growth temperatures were used according to respective enzymes being expressed. Enzymes were produced at 37 °C. At the end of protein expression, cells were pelleted by centrifugation at 4000 x *g* for 15 min. The cell pellets were stored at - 80 °C prior to enzyme purification. For expressing TsER TB auto induction media was used.

Preparation of buffers for Äkta purifier

Binding buffer: 50 mM KPi, 20 mM imidazole, 0.5 M NaCl, 10 % (w/v) glycerol in ddH₂O, adjusted with HCl to pH 8. The solution was filtered through 0.45 μm filter paper prior to use.

Elution buffer: 50 mM KPi, 500 mM imidazole, 0.5 M NaCl, 10 % (w/v) glycerol in ddH₂O, adjusted with HCl to pH 8. The solution was filtered through 0.45 μm filter paper prior to use.

Desalting buffer: KPi, and Tris-HCl buffer with different concentration and pH were used throughout this study.

Cell disruption by sonication

All cell disruption in this study was performed by sonication. Cell pellet [10 % (w/v) to 20 % (w/v)] was dissolved in the binding buffer. DNase 5 $\mu\text{g}\cdot\text{mL}^{-1}$ and 1 mM MgCl₂ were added to the solution. The cell suspension in a 50 mL falcon tube was placed in ice/water and a sonotrode was inserted to the cell suspension. Sonication was performed for 20 min (0.5 s cycle and 80 %). Cell suspension was centrifuged at 20.000 x *g* for 30 min at room temperature. In the following SsGDH was heat treated in a water bath at 70 °C for 30 min before centrifugation. This step leads to a significant activation and purification. The supernatant was filtered through 0.45 μm filter before application to an Äkta purifier.

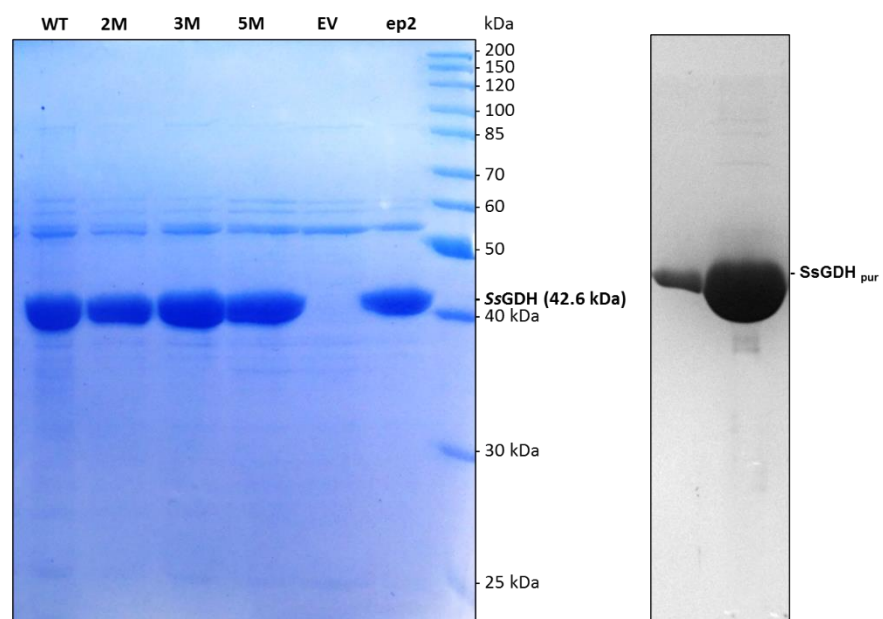


Figure S2 SDS-PAGE analysis of SsGDH variants after cell lysis (left) and after purification (right) (WT = natural origin, M = Mutant generation, ep2 = intermediate variant from error prone approach)

Size exclusion chromatography (SEC)

SEC was used to remove imidazole and salt in the elution buffer. A 50 mL desalting column was applied to the Äkta purifier. Buffer of interest (desalting buffer) depending on the enzymes were used to equilibrate the column. Approximately 100 mL of a desalting buffer would be needed. A protein eluate from the previous IMAC purification was loaded to the desalting column. Maximum volume of 15 mL could be loaded to allow good separation. Upon loading, desalting column was loaded to the column with 10 mL \cdot min⁻¹ flow rate. A single fraction of protein in a desired desalting buffer was collected. The column was equilibrated with 100 mL of desalting buffer and ready for

the next protein elution. Salts and buffer of the elution buffer would be removed from the column during column equilibration.

Determination of enzyme concentration

Enzyme concentrations were determined using either Bradford assay (BioRad) or by UV-Vis spectroscopy using extinction coefficients calculated by ExPASy ProtParam tool.

Measurements of kinetic constants

Kinetic measurements were performed in MTP format. Reaction conditions: 100 mM Tris-HCl pH 8.0, 65 °C. Enzyme concentration was set to 0.1 mg·mL⁻¹ for all measurements.

Equation (I) Michaelis-Menten:

$$Y = \frac{v_{max} \cdot X}{K_m + X}$$

Equation (II) Substrate-Inhibition:

$$Y = \frac{v_{max} \cdot X}{[K_m + X \cdot (1 + \frac{X}{K_i})]}$$

Enzyme Engineering and mutagenesis

Single-site saturation mutagenesis. partially overlapped primer approach.

Saturation mutagenesis

To construct mutagenesis libraries, PCRs (each 50 µL) were prepared with 2.5 µL forward primer and reverse primer (10 µM stock), 30 - 50 ng of template plasmid DNA, 1 U of Phusion DNA polymerase (New England Biolabs GmbH, Frankfurt am Main), 10 µL of 5x Phusion HF buffer, 1 µL of dNTPs (each 10 mM) and 5 µL DMSO to reduce fidelity. PCR was run at 98 °C for 1 min, followed by 16 - 18 cycles at 98 °C for 5 s, 65 °C for 30 s, and 72 °C for 3.5 min. A final elongation step was performed at 72 °C for 10 min. Afterwards PCR reactions were incubated over night with 20 U *DpnI* at 37 °C. Chemically competent *E. coli* BL21 (DE3) (RbCl method) were then transformed with 10 µL of digested PCR mixtures. Primers (Eurofins Genomics Germany GmbH, Ebersberg) were designed to not completely overlap.⁴

Table S0 Primers used for creating site saturation mutagenesis.

Name	5'→ 3' oligo sequence
F_SsGDH_G40NNK	GGTATTTCGNKACCGATCGTGAAATTGTGAATGGTAAACTGAC
R_SsGDH_G40MNN	CACAATTTACGATCGGTMNNGCAAATACCATTATAAATGGTGCG
F_SsGDH_T41NNK	AATGGTATTTGCGCENKATCGTGAAATTGTGAATGG
R_SsGDH_T41MNN	CACGATCMNNGCCGCAAATACCATTATAAATGGTGCGAA
F_SsGDH_E44NNK	GGGTCAGTTTACCATTACAATMNNACGATCGGTGCCGC
R_SsGDH_E44MNN	GCGGCACCGATCGTNNKATTGTGAATGGTAAACTGACCC
F_SsGDH_K133NNK	GATCCGNNKTATCTGGTAAAATCCGAAAAGCATTGAAG
R_SsGDH_K133MNN	CAGATAMNNGGATCATCATACCACCATTCACGCATAAAG
F_SsGDH_D176NNK	CCTGTGATNNKGGCACCCGTAATTGTCTGTAAGTTCTGG
R_SsGDH_D176MNN	GGTGCCMNNATCACAGGTCCAAACCGGAACACGTTTCTG
F_SsGDH_T189NNS	GGTTGTTGGCNSGGTCCGATTGGTGTCTGTTTACCCTG
R_SsGDH_T189SNN	CCAATCGGACCSNNGCCAACAACAGAACTTTACGACAATTC
F_SsGDH_G190NDT	GTTGGCACCNNTCCGATTGGTGTCTGTTTACCCTGCTG
R_SsGDH_G190NDT	ACACCAATCGGAHNGGTGCCAACAACAGAACTTTACGAC
F_SsGDH_P191NDN	GAGTTNDNTCATCACAAGTCCACACTGGAACCCCTTTTCTG
R_SsGDH_P191NDN	GTGATGANDNAACTCTAAATTGTAGGAAAGTTCTCG
F_SsGDH_I192NNK	GGTTGTTGGCACCGGTCCGNNKGGTGTCTGTTTACCCTGC
R_SsGDH_I192MNN	GCAGGGTAAACAGAACACCMNNGGACCGGTGCCAACAACC
F_SsGDH_N211NNK	GTTTGGATGGCANNKCGTCTGAACCGACCGAAGTTGAAC
R_SsGDH_N211MNN	CACGACGMNNTGCCATCCAACCTCCAGACCATAGGTACG
F_SsGDH_R212NNK	GTTTGGATGGCAAACNNKAGAGAACCCACTGAG
R_SsGDH_R212MNN	CTCAGTGGGTTCTCTTGMNNTGCCATCCAAAC
F_SsGDH_R213NNK	GGCAAATCGTNNKGAACCGACCGAAGTTGAACAGACCG
R_SsGDH_R213MNN	CGGTTMNNACGATTTGCCATCCAACCTCCAGACCATAG
F_SsGDH_P215NNK	GGATGGCAAACAGAGAANNKACTGAGGTAGAACAG
R_SsGDH_P215MNN	CTACCTCAGTNNKTTCTCTTCTGTTTCCATCCAAACC
F_SsGDH_A253NNK	GATGTGATTATTGATNNKACCGGTGCCGATGTTAATATTCTGGGCAATG
R_SsGDH_A253MNN	CATCGGCACCGGTMNNATCAATAATCACATCAAATTTGCCACGCTATC
F_SsGDH_T254NNK	ACTCAGTAGGTAAGTTCGATGTAATAATAGACGCANNKGGAGCAGATGTAATATATTA
R_SsGDH_T254MNN	TGAGTCATCCATTCAAGCTACATTATTATCTGCGTNNMCCCTCGTCTACATTATATAAT
F_SsGDH_G255NNS	TTGATGCAACCNNSGCCGATGTTAATATTCTGGGCAATG
R_SsGDH_G255SNN	CATCGGCSNNGGTTGCATCAATAATCACATCAAATTTGC
F_SsGDH_F277NNK	TCTGGGTCTGNNKGGTTTTAGCACCTCTGGTAGCGTTC
R_SsGDH_F277MNN	TGCTAAAACCMNNGACACCCAGAACCATTACGACCC
F_SsGDH_G278NNK	GTCTGTTTNNKTTTAGCACCTCTGGTAGCGTTCGCTG
R_SsGDH_G278MNN	CCAGAGGTGCTAAAMNNAACAGACCCAGAACCATT
F_SsGDH_F279NNK	GGT CTG TTT GGT NNK AGC ACC TCT GGT AGC GTT CCG
R_SsGDH_F279MNN	CC AGA GGT GCT MNN ACC AAA CAG ACC CAG AAC ACC
F_SsGDH_S280NNK	TTGGTTTTNNKACCTCTGGTAGCGTTCGCTGGAT
R_SsGDH_S280MNN	GCTACCAGAGGTMNNAACCAAACAGACCCAGAACAC
F_SsGDH_T281NNK	GGTTTTAGCENKCTCTGGTAGCGTTCGCTGGATTA
R_SsGDH_T281MNN	CGCTACCAGAMNNGCTAAAACCAAACAGACCCAGAA
F_SsGDH_L305NNK	ACCATTATTGGCENKGTGAATGGTCAGAAACCGCA
R_SsGDH_L305MNN	CTGACCATTACMNNGCCAATAATGGTTTTATTGGTATG
F_SsGDH_V306NNK	GGCCTGNNKAATGGTCAGAAACCGCATTTTCAGC
R_SsGDH_V306MNN	CTGACCATTAATCAGGCCAATAATGGTTTTATTGG
F_SsGDH_K354NNK	TTGATTTCCGCATGTCTNNKTTACGCGACACTTTTCAG
R_SsGDH_K354MNN	CTGAAAGTGCTGCGTGAAAGAMNNCATGGCGAAATCAA

error prone PCR

To introduce random point mutations into a gene, the method of error-prone PCR (epPCR) was used. The GoTaq® DNA polymerase is used for this purpose. This has no 3'→5' proofreading activity, resulting in an average of 8×10^{-6} to 2×10^{-4} errors per nucleotide^{5,6} (Eckert & Kunkel 1990; Cline et al. 1996). This error rate can be modified by using unequal concentrations of the different deoxynucleotides^{7,8}, increased concentrations of $MgCl_2$, and by the addition of $MnCl_2$ can be further increased⁹. A standard epPCR was done according to the protocol of Sperl¹⁰ and contained 0.35 mM dATP, 0.4 mM dCTP, 0.2 mM dGTP, 1.35 mM dTTP as well as 0.75 mM $MnCl_2$, 1 mM $MgCl_2$, 1 μ M of each primer (T7 and T7term), ~ 100 ng of template, DNA Green GoTaq® buffer (also containing $MgCl_2$) and 20 U of GoTaq® DNA-Polymerase (Promega). Reaction mixtures were initially heated to 95 °C for 5 min followed by 28 cycles of 30 s at 95 °C, 30 s at 60 °C, 45 sec at 72 °C and a final elongation step at 72 °C for 5 min. Reactions were purified using a PCR clean-up kit (Macherey-Nagel) and digested using the restriction enzymes *Xba*I and *Bsa*I (1 h at 37 °C). A standard ligation into pET28b-*ssgdh* backbone was performed at 12 °C o.n.

Screening procedure

Chemical competent *E. coli* BL21 (DE3) cells¹¹ were transformed with pET28a-*ssgdh* mutagenesis libraries and plated on LB-Kan₅₀ plates. Single colonies were transferred into 96 deep-well plates containing 1.2 mL auto-induction medium supplemented with 50 μ g·mL⁻¹ kanamycin and were then incubated at 37 °C for 20 h at 1000 rpm. 50 μ L aliquots of each well was mixed with 50 μ L of 60 % glycerol and were stored in a separate plate at -80 °C as backup. After centrifugation of the DWPs (15 min, 4 °C, 4000 x g), the supernatants were discarded, and the cell-pellets were resuspended in lysis buffer (2.5 mg·mL⁻¹ lysozyme, and 0.1 mg·mL⁻¹ DNaseI in 100 mM Tris-HCl pH 8) and incubated at 37 °C for 1 h at 1000 rpm. After heat incubation in a water bath (70 °C for 30 min), disrupted cells were centrifuged at 4 °C for 30 min at 4000 x g. After that photometric activity measurements were performed at 358 nm for 1 h at 45 °C, respectively. For that 20 μ L of supernatant were added to 180 μ L master mix containing 10 mM P2NA⁺ or P4NA⁺ or P5NA⁺ and 50 mM D-glucose in 100 mM Tris-HCl pH 8. Analyses were performed by calculating increases of absorption over time. Variants with residual activity greater than the wild-type enzyme plus standard deviation were considered hits. Controls included empty vector controls, medium controls, and wild-type controls.

HPLC-Analysis

The concentrations of D-glucose for NA2NA²⁺ correlated reactions were analyzed using an HPLC system (Shimadzu, Kyoto, Japan or Dionex®, Sunnyvale, USA) equipped with a Rezex™ ROA-H+ organic acid column (300 mm x 7.8 mm; Phenomenex®, Torrance, USA). Sulfuric acid (2.5 mM) was used for eluent with a flow rate of 0.5 mL·min⁻¹ at 70 °C. The reactant was determined by a refractive index detector (RID). Samples at different time points were taken from 1 mL reactions containing 0.5 mg mL⁻¹ SsGDH variant, 50 mM D-Glucose, 10 mM NA2NA²⁺, 100 mM Tris-HCl pH 8.0 incubated at 45 °C at 700 rpm (Eppendorf Thermoblock) and filtered (12000 x g for 10 min) with 10 kDa spin filters (VWR).

Biocatalytic conversion of ketoisophorone

Turnover by SsGDH variants was shown via a cofactor regeneration system. 100 μ g·mL⁻¹ SsGDH, 50 mM – 100 mM glucose, 170 μ g·mL⁻¹ TsER, 2 mM - 10 mM ketoisophorone in 50 mM Tris-HCl (pH 7.5) containing 5 mM $CaCl_2$ were prepared. In addition, 5 mM - 9 mM of the cofactor (MNA⁺, BNA⁺, P2NA⁺, P4NA⁺, P5NA⁺), was added. As a positive control, 0.2 mM NADP⁺ was used instead of the biomimetic. In addition, negative controls were prepared without cofactor, SsGDH, and TsER, respectively. The reaction mixtures were incubated for 40 h at 45 °C and 300 rpm and subsequently analysed by GC-FID.

GC-Analysis

For extraction of the biocatalysis samples from section above, 1 mL MTBE (2-methoxy-2-methylpropane) was added to each of the 500 μL preparations, shaken and then centrifuged (12000 $\times g$, 1 min). 500 μL of the supernatant was now transferred to new reaction tubes and a spatula tip of MgSO_4 was added to each to dry the samples. After the addition of MgSO_4 , the mixtures were again centrifuged (12000 $\times g$, 1 min) and 200 μL of the supernatant was transferred to microvials. A GC-2010 Plus high-end gas chromatograph from Shimadzu was used for analysis with a MEGA β -DEX DAC column (25 m, 0.25 mm, 0.25 μm ; BGB Analytics, Germany) to separate enantiomers. 1 μL of sample was injected with a split of 13. Helium was used as the carrier gas. The injector and detector temperature were 250 $^\circ\text{C}$. The oven temperature was maintained at 80 $^\circ\text{C}$ for 1.5 min and then was increased at a rate of 10 $^\circ\text{C min}^{-1}$ to 155 $^\circ\text{C}$ and held for 2 min.

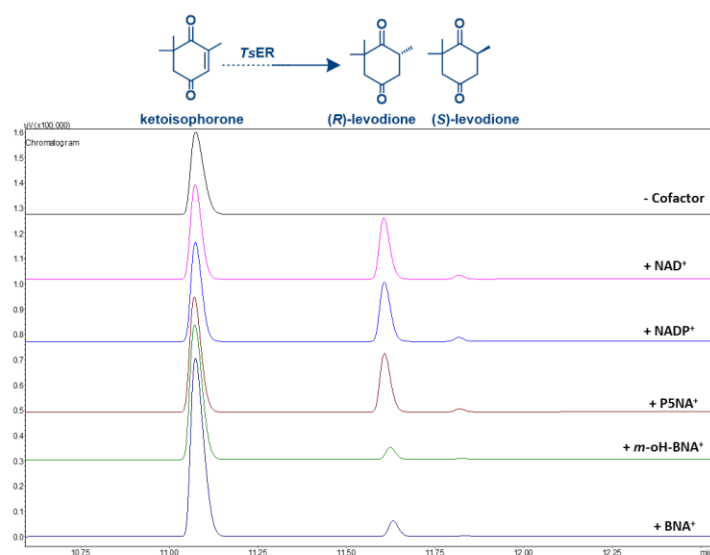


Figure S3 Exemplary GC-FID chromatograms for analysis of biocatalytic levodione production.

Table S1 Activity measurement of SsGDH variants derived from semi-rational designs in $U \cdot g^{-1}$. Reaction conditions: 50 mM cofactor, 2 mM D-glucose, 65 mM Tris-HCl pH 8 (at RT), 45 °C, 1 mg mL⁻¹ purified enzyme.

	I192T/G40S	I192T	T254R/G255P	I192T/T281K	I192T/T41A	I192T/V306I (2M)	I192T/P191H	G40Q/V306I	I192C	I192T/F279S	I192T/V306I/E44D (3M)	E44D/D176G/I192T/ A253T/V306I (5M)
MNA ⁺	2	2	0	1	2	3	3	2	2	1	4	0
BNA ⁺	16	14	0	5	4	22	6	11	8	0	21	63
P2NA ⁺	16	13	0	5	11	47	3	26	9	1	59	129
P4NA ⁺	22	20	0	7	10	52	4	30	12	0	58	180
P5NA ⁺	29	21	0	8	11	47	4	26	13	0	54	202
NA2NA ²⁺	9	8	0	3	3	14	5	4	6	1	18	2

Screening

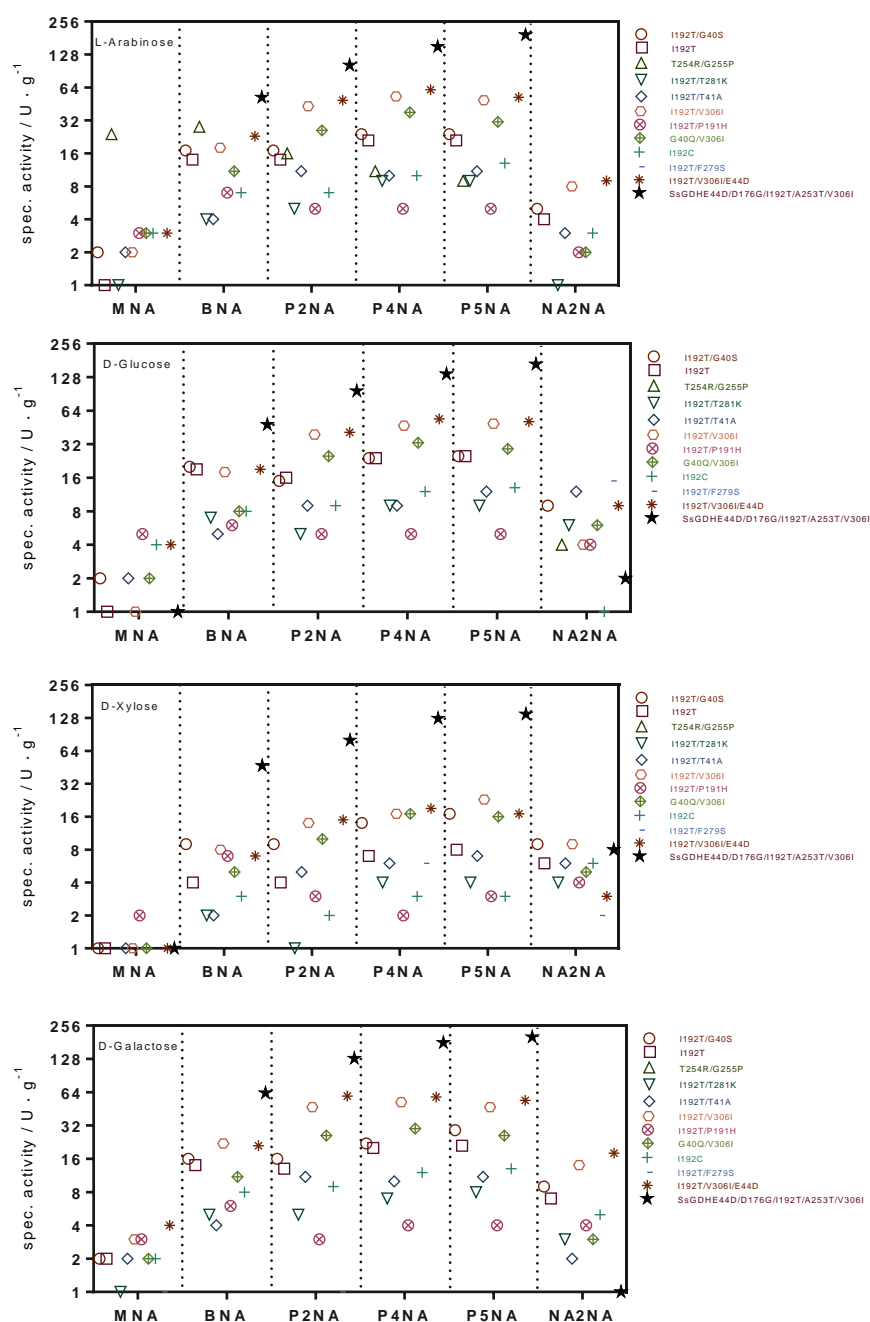


Figure S4 Activity measurement of SsGDH variants. Activities are plotted on a log₂ scale. Reaction conditions: 50 mM cofactor, 2 mM aldose substrate, 65 mM Tris-HCl pH 8 (at RT), 45 °C, 1 mg mL⁻¹ purified enzyme.

Screening

In the following **Table S2** we give the corresponding values to the single point activity measurements in **Figure 1** of the main part with the reaction conditions: 65 °C, pH 7, 50 mM aldose substrate, 9 mM cofactor, 0.1 mg · mL⁻¹ of the respective enzyme variant.

Table S2 Activity measurement of SsGDH variants 3M and 5M with different sugars and cofactors in U · g⁻¹.

SsGDH WT	MNA⁺	+/-	BNA⁺	+/-	P2NA⁺	+/-	P4NA⁺	+/-	P5NA⁺	+/-	NA2NA²⁺	+/-
D-Glucose	n.d.		2	0.8	5	1.0	5.5	0.2	5.5	0.2	2	0.2
D-Xylose	n.d.		4	1.0	5	0.5	7	2.0	7	0.1	3	0.8
L-Arabinose	n.d.		3	0.5	5	0.4	5	0.4	5	0.3	2	0.1
D-Galactose	n.d.		2	0.2	5	0.1	6	0.1	6	0.2	1	0.2

SsGDH 3M	MNA⁺	+/-	BNA⁺	+/-	P2NA⁺	+/-	P4NA⁺	+/-	P5NA⁺	+/-	NA2NA²⁺	+/-
D-Glucose	1	0.1	29	1.0	50	1	64	2	72	2	19	2
D-Xylose	1	0.1	21	1.0	38	1	48	2	52	1	12	2
L-Arabinose	1	0.1	22	2.0	38	1	49	1	50	1	15	2
D-Galactose	1	0.1	17	1.0	31	1	39	1	47	2	13	1

SsGDH 5M	MNA⁺	+/-	BNA⁺	+/-	P2NA⁺	+/-	P4NA⁺	+/-	P5NA⁺	+/-	NA2NA²⁺	+/-
D-Glucose	1	0.1	48	1	96	2	137	3	167	4	26	1
D-Xylose	2	0.2	47	1	81	3	127	1	140	1	23	3
L-Arabinose	1	0.1	53	2	103	5	151	1	194	1	27	1
D-Galactose	1	0.1	63	1	130	9	180	2	203	10	4	2

Table S3 Improvement-Matrix for various substrate-cofactor combinations comparing 5M vs. 3M and 5M vs. WT.

Ratio 5M:3M	MNA⁺	BNA⁺	P2NA⁺	P4NA⁺	P5NA⁺	NA2NA²⁺
D-Glucose	1.4	1.6	1.9	2.1	2.3	1.4
D-Xylose	2.5	2.2	2.2	2.6	2.7	2.0
L-Arabinose	0.9	2.4	2.7	3.1	3.9	1.8
D-Galactose	1.3	3.6	4.2	4.6	4.3	0.3

Ratio 5M:WT	MNA⁺	BNA⁺	P2NA⁺	P4NA⁺	P5NA⁺	NA2NA²⁺
D-Glucose	NaN	24	19	25	30	13
D-Xylose	NaN	12	16	18	20	8
L-Arabinose	NaN	18	21	30	39	14
D-Galactose	NaN	32	26	30	34	4

3M= E44D, I192T, V306I

5M= E44D, D176G, I192T, A253T, V306I

Kinetics

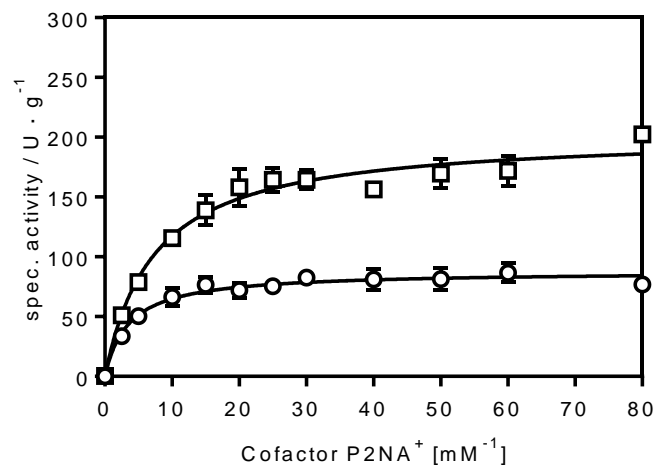


Figure S5 Kinetic measurement of SsGDH (○) SsGDH_{E44D/I192T/V306I} (3M) and (□) SsGDH_{E44D/D176G/I192T/A253T/V306I} (5M) with varying P2NA⁺ cofactor concentration. Reaction conditions: 100 mM Tris-HCl pH 7.0, 65 °C, 50 mM D-glucose, SsGDH Variant 0.1 mg · mL⁻¹

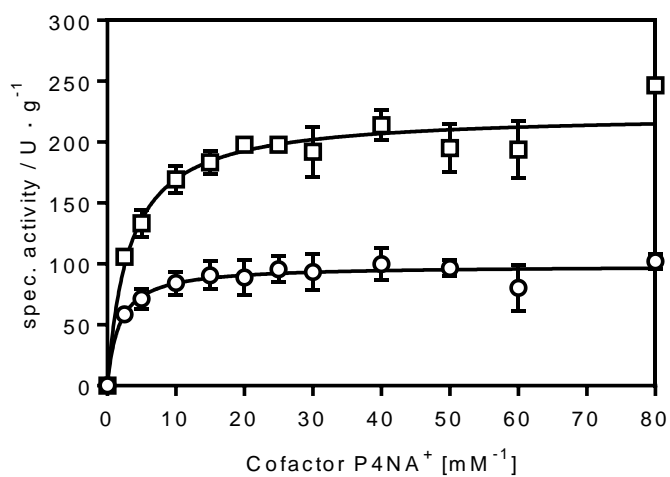


Figure S6 Kinetic measurement of SsGDH (○) SsGDH_{E44D/I192T/V306I} (3M) and (□) SsGDH_{E44D/D176G/I192T/A253T/V306I} (5M) with varying P4NA⁺ cofactor concentration. Reaction conditions: 100 mM Tris-HCl pH 7.0, 65 °C, 50 mM D-glucose, SsGDH Variant 0.1 mg · mL⁻¹

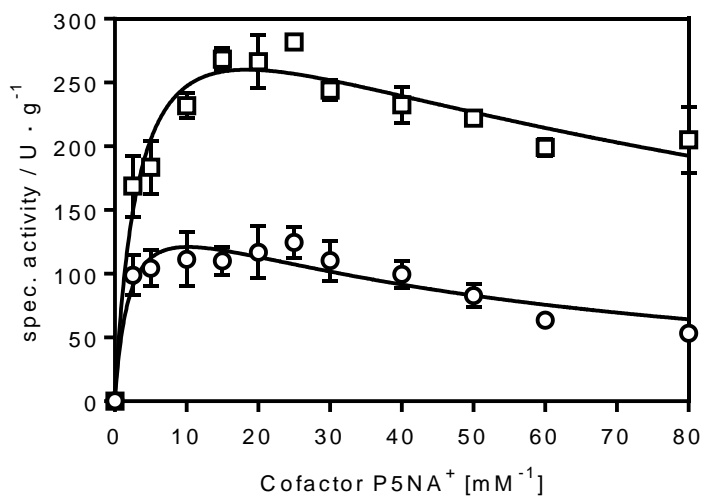


Figure S7 Kinetic measurement of SsGDH (○) SsGDH_{E44D/I192T/V306I} (3M) and (□) SsGDH_{E44D/D176G/I192T/A253T/V306I} (5M) with varying P5NA⁺ cofactor concentration. Reaction conditions: 100 mM Tris-HCl pH 7.0, 65 °C, 50 mM D-glucose, SsGDH Variant 0.1 mg · mL⁻¹

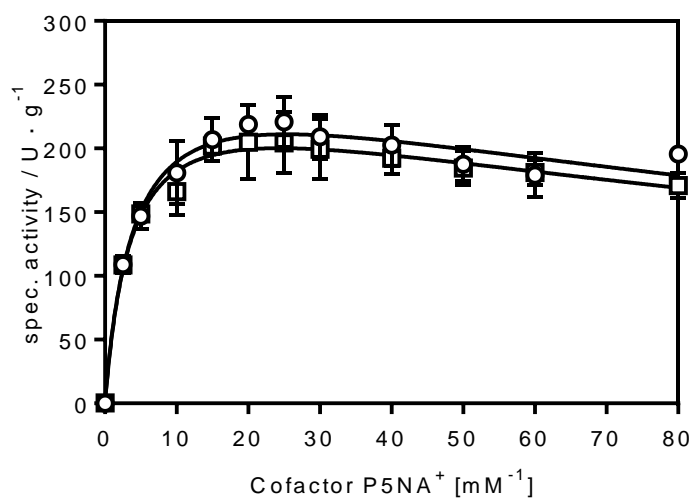


Figure S8 Comparison of kinetic measurement of SsGDH 5M with 50 mM (○) D-glucose or (□) D-galactose as substrate with varying P5NA⁺ cofactor concentration. Reaction conditions: 100 mM Tris-HCl pH 7.0, 65 °C, SsGDH Variant 0.1 mg · mL⁻¹

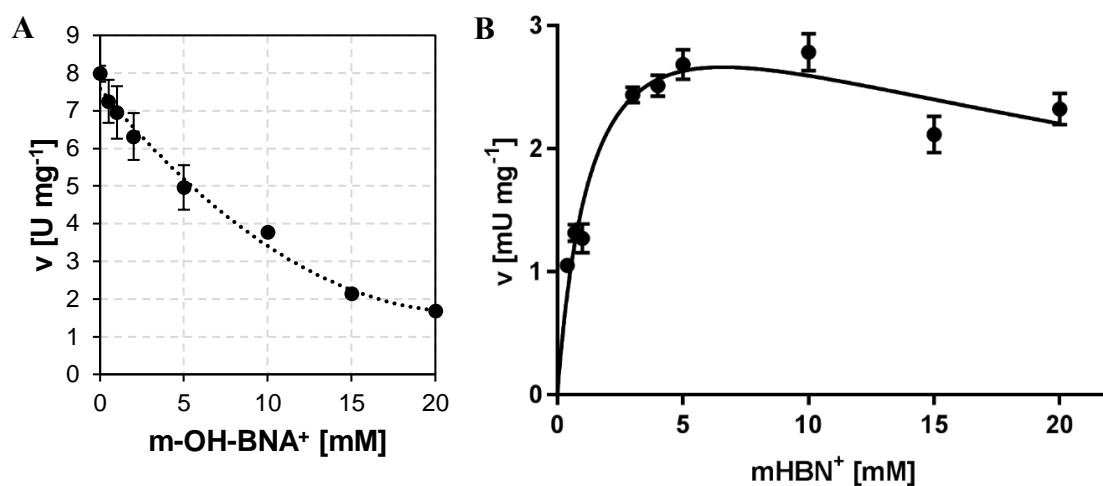


Figure S9 (A) Inhibition study of SsGDH 2M with meta-OH-BNA⁺ at constant NAD⁺ concentration. Activity in U mg⁻¹ as absorbance increase at 340 nm and at 65 °C. **(B)** Kinetics of SsGDH 2M with meta-OH-BNA⁺ (mHBN⁺) and 50 mM glucose at pH 9.5 and 65 °C.

Table S3 Kinetic constants for the redesigned biocatalysts and different substrates.

	Aldose	Cofactor	V_{max} [U g ⁻¹]	K_m cofactor [mM]	K_i cofactor [mM]
SsGDH DTI (3M)	D-glucose	P2NA ⁺	88 ± 2	3.6 ± 0.5	/
		P4NA ⁺	99 ± 3	1.7 ± 0.4	/
	D-galactose	P5NA ⁺	172 ± 21	2.1 ± 0.8	49 ± 14
SsGDH DGTTI (5M)	D-glucose	P2NA ⁺	203 ± 5	7.3 ± 0.8	/
		P4NA ⁺	224 ± 5.5	3.2 ± 0.5	/
		P5NA ⁺	280 ± 18	4.1 ± 0.8	156 ± 41
	D-galactose	P5NA ⁺	358 ± 25	3.5 ± 0.7	98 ± 21

Docking Studies

Docking was done in Yasara via the macro dock_run.mcr.

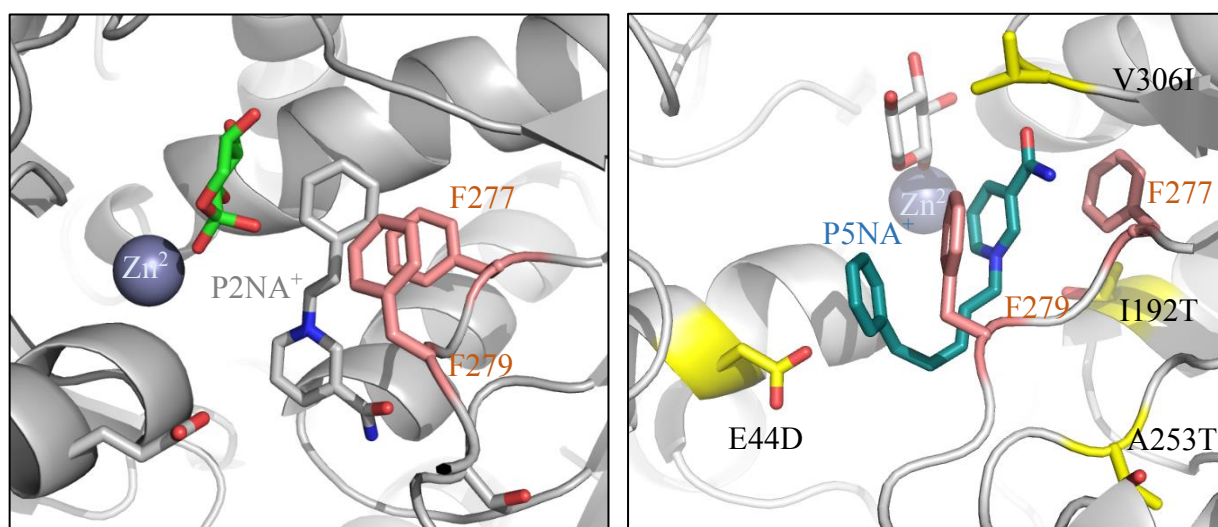


Figure S10 Active site view of SsGDH WT and 5M (pdb: 2cdc_A) with bound sugar substrate D-xylose (green) and cofactor biomimetic (A) P2NA⁺ (grey) in a non-favorable orientation π - π -stacked in between F277 and F279 (salmon) as well as (B) biomimetic P5NA⁺ (turquoise) in a predicted binding state.

Spectral analysis of enzymatically reduced cofactors

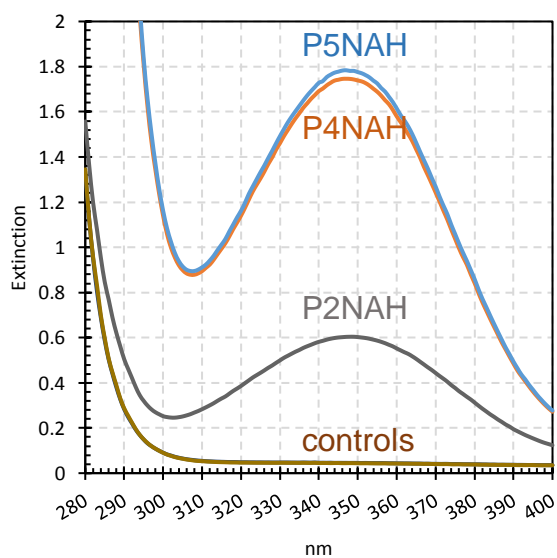


Figure S11 Spectral analysis of enzymatically reduced cofactors P2NA⁺, P4NA⁺ and P5NA⁺ with absorption maxima at 348 nm. Controls were made without addition of cofactor or D-glucose, respectively. (No conclusions should be drawn from the peak areas since different cofactor concentrations were plotted).

Effect of pH on biomimetic nicotinamide cofactors.

To ensure that the increase in absorbance at 358 nm was due to the activity of the enzymes containing biomimetic nicotinamide cofactors, the effect of pH on the stability of the small cofactors was previously investigated. Figure 7A shows the increase in absorbance over time of oxidized biomimetic nicotinamide cofactors at 358 nm as affected by pH. The amount of oxidized cofactor used was always 10 μmol . In particular, the cofactors BNA⁺ and P5NA⁺ were affected by an alkaline environment. The pH effect on the stability of BNA⁺ became evident from a pH of 9.0 and reached a maximum of $1.72 \pm 0.11 \text{ mAU min}^{-1}$ at pH 10.5, whereas an influence on P5NA⁺ occurred from a pH of 8.5 and increased up to an absorption increase of $6.34 \pm 0.06 \text{ mAU min}^{-1}$ at pH 10.5. In descending order, the pH effect on cofactors P3NA⁺, P2NA⁺, and P5NA⁺ was extremely small in the basic pH range, as there was no significant increase in absorbance at 358 nm. In the acidic environment, all cofactors were stable as no increase in absorbance was observed. Figure 7B shows the decrease of the reduced cofactor BNAH under the influence of pH. When looking at the stability of BNAH at different pH, it was noticeable that the reduced cofactor was much more unstable than the oxidized one. Especially in strongly acidic environments at pH 3.0 to 7.0, the decrease of BNAH was very high. The maximum was $17.0 \pm 0.1 \text{ nmol min}^{-1}$ BNAH at pH 3.5, which meant that all BNAH was degraded after just 6 min. In the alkaline environment, there was no decrease in BNAH, thus the cofactor was stable at pH 7.5 - 10.5. In summary, pH had little effect on the stability of cofactors P2NA⁺, P3NA⁺, and P5NA⁺ in the range of pH 3.0 to 10.5, whereas cofactors BNA⁺ and P5NA⁺, respectively, were stable in the pH range between 3.0 and 8.5 and 8.0. While in the alkaline environment, an effect of pH on BNA⁺ and P5NA⁺ was observed.

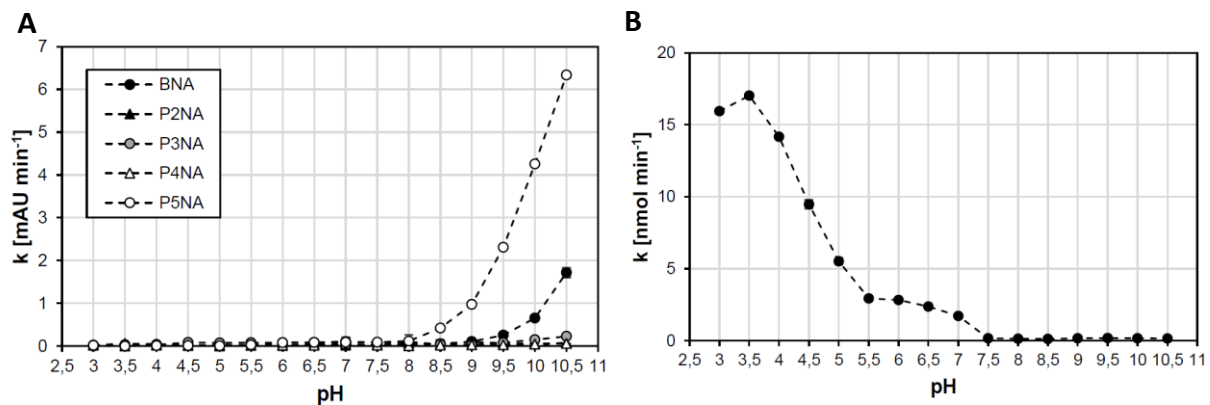


Figure S12 Temporal absorbance change k of (A) oxidized biomimetic nicotinamide cofactors as influenced by pH at 45 °C and an initial amount of 10 μmol . (B) BNAH under the influence of pH at 45 °C and at an initial amount of 100 nmol.

Sequences

>SsGDH-5M

```

ATGAAAGCCATTATTGTGAAACCTCCGAATGCCGGTGTTCAGGTTAAAGATGTGGATGAAAAAACTGGATAGCTATGG
CAAAATTAATTCGCACCATTTATAATGGTATTTGCGGCACCGATCGTGATATTGTGAATGGTAAACTGACCCTGAGCAC
CCTGCCGAAAAGGTAAAGATTTCTGGTGCTGGGTATGAAGCAATTGGTGTGGGAAGAAAGCTATCATGGTTTTAGCC
AGGGTGATCTGGTTATGCCGGTAAATCGTCGTGGTTGGTATTTGTCGTAATTGTCTGGTTGGTCCGCGATTTTTGTGA
AACCGGTGAATTTGGTGAAGCCGGTATTCATAAAATGGATGGCTTTATGCGTGAATGGTGGTATGATGATCCGAAATATCT
GGTGAATTTCCGAAAAGCATTGAAGATATTGGTATTCTGGCACAGCCGCTGGCAGATATTGAAAAATCCATTGAAGAAA
TTCTGGAAGTGAGAAACGTGTTCCGGTTTGGACCTGTGATGGTGGCACCCCTGAATTGTCGTAAGTTCTGGTTGTTGGCA
CCGGTCCGACGGGTGTTCTGTTTACCTTGCTGTTTCGTACCTATGGTCTGGAAGTTTGGATGGCAAATCGTCGTGAACCGA
CCGAAGTTGAACAGACCGTTATTGAAGAAACCAAAACCAATTATTATAATAGCAGCAATGGCTATGATAAACTGAAAGAT
AGCGTGGGCAAATTTGATGTGATTATTGATACAACCGGTGCCGATGTTAATATTCTGGGCAATGTTATTCCGCTGCTGGGT
CGTAATGGTGTCTGGGTCTGTTTGGTTTTAGCACCTCTGGTAGCGTTCCGCTGGATTATAAAACCTGCAGGAAATTGTTT
ATACCAATAAAACCAATTATTGGCCTGATTAATGGTTCAGAAACCGCATTTTCAGCAGGCAGTTGTTTCATCTGGCAAGCTGGA
AAACCGTGTATCCGAAAGCAGCAAAAATGCTGATTACCAAAACCGTGAGCATTAAATGATGAAAAAGAACTGCTGAAAGTG
CTGCGTGAAAAAGAACATGGCGAAATCAAATTCGTATTCTGTGGAAAGCGGGAGACCTGTGCTGGGCAGCAGCCACC
ACCACCACCACCTAA

```

Appendix NMR Spectra of biomimetic cofactors

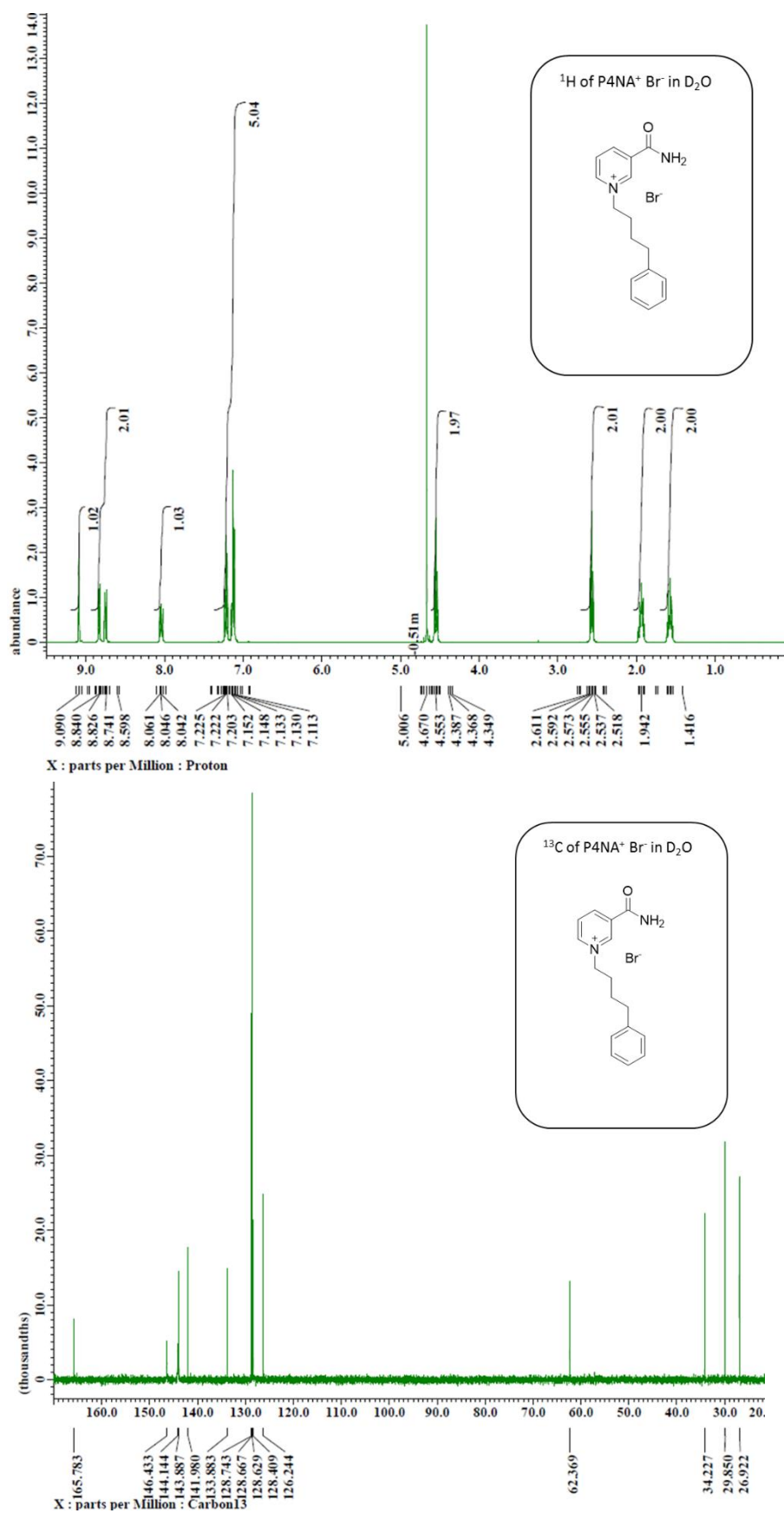


Figure S13 ^1H and ^{13}C NMR spectra of P4NA in D $_2$ O

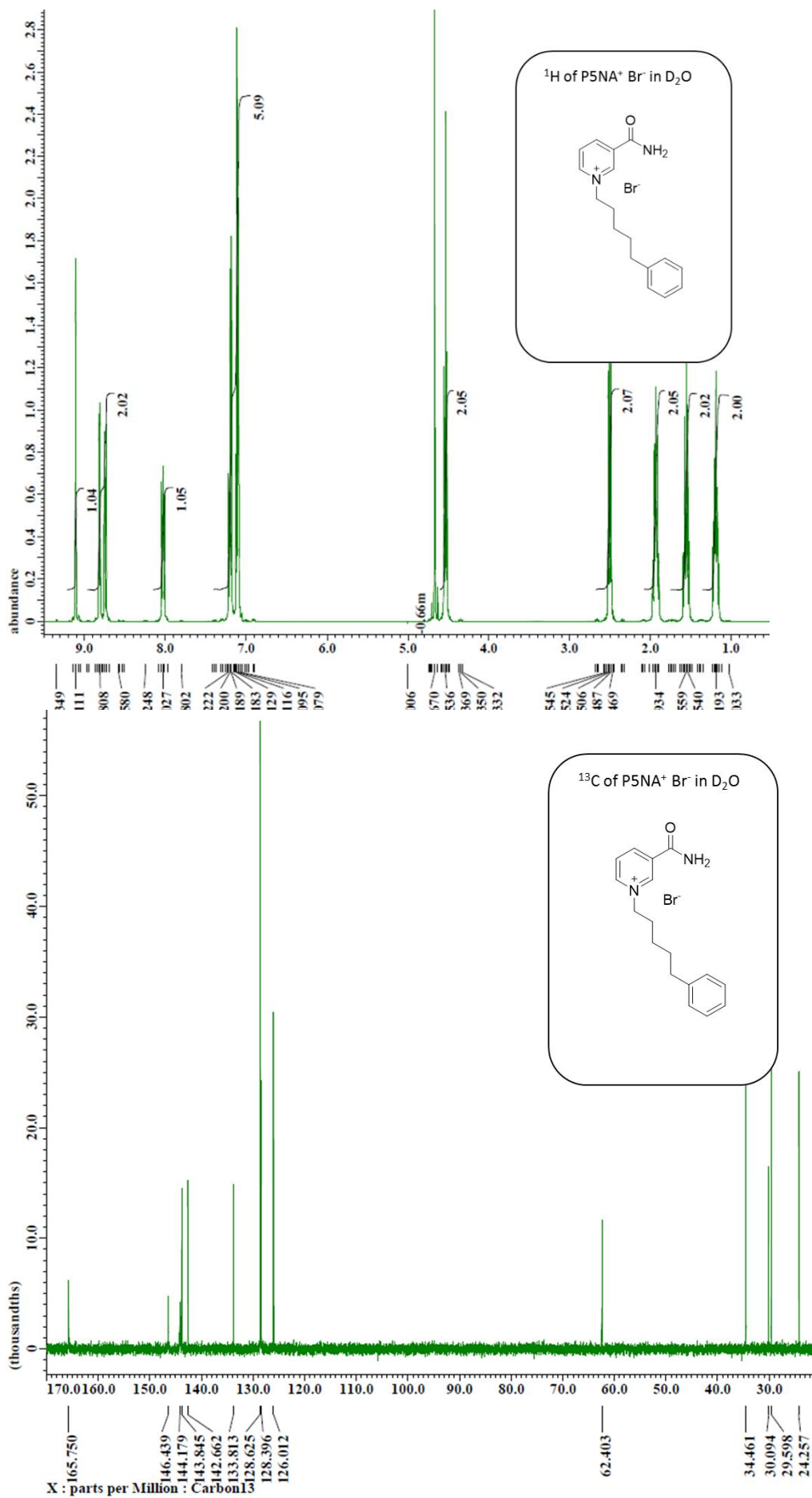


Figure S14 ¹H and ¹³C NMR spectra of P5NA in D₂O

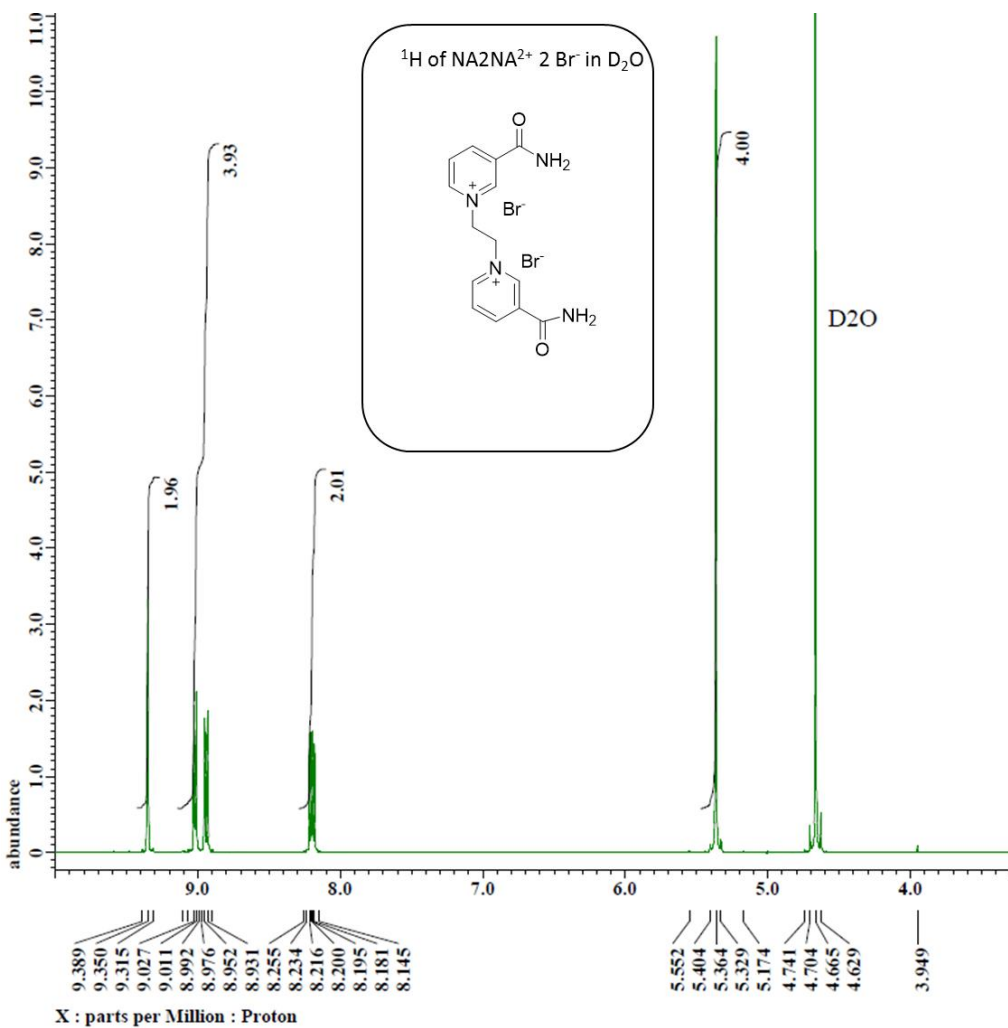
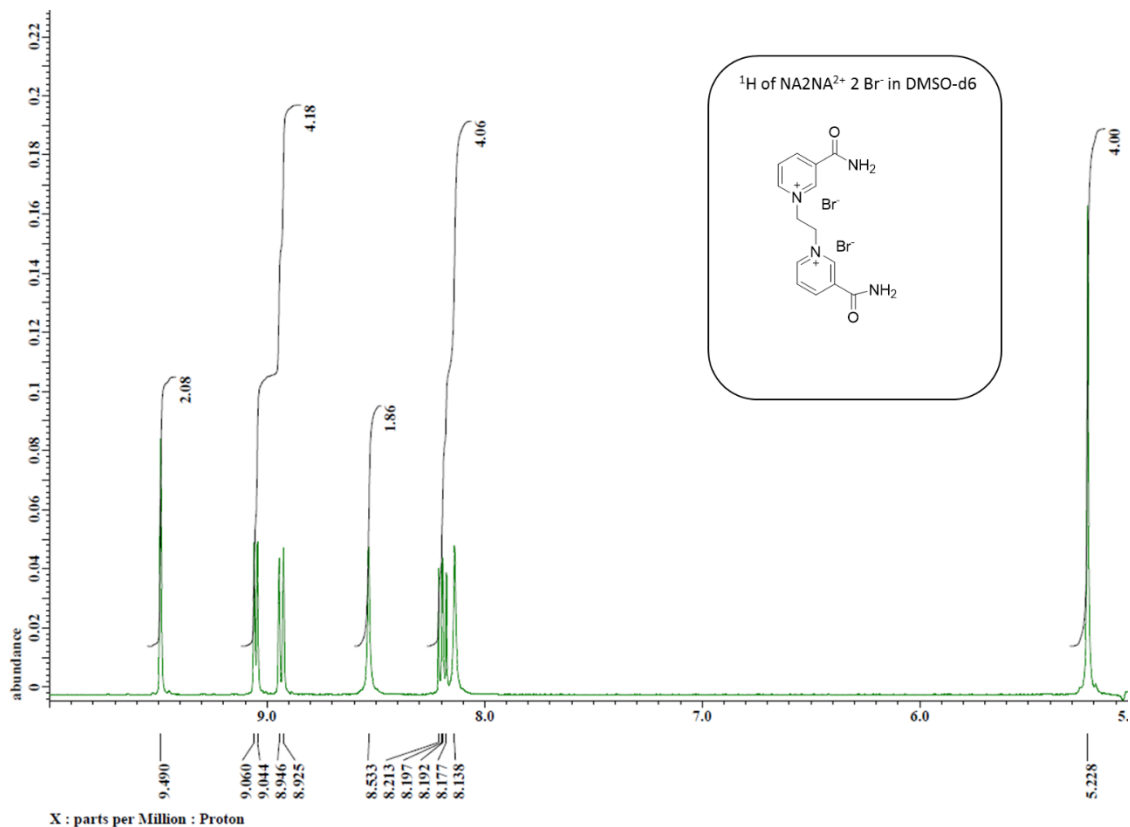


Figure S15 ¹H NMR spectra of NA₂NA in DMSO-d₆ and D₂O

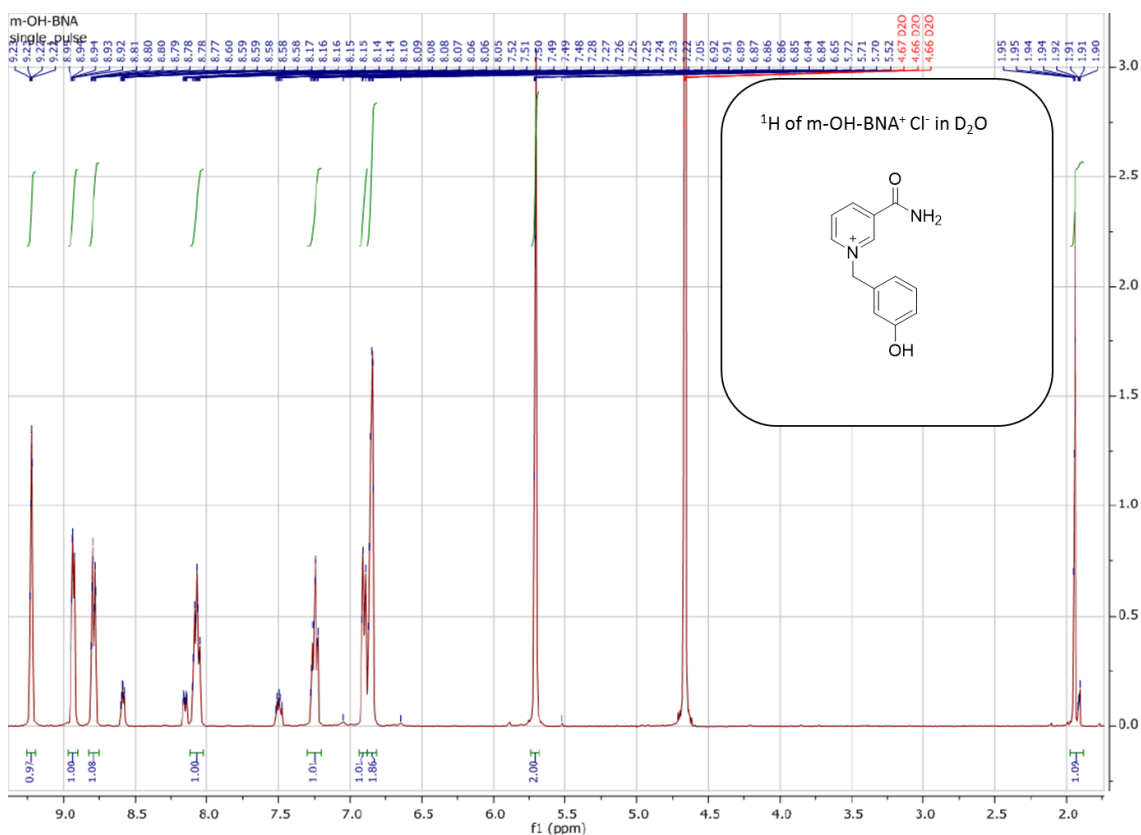


Figure S16 ¹H NMR spectra of m-OH-BNA in D₂O

References

- (1) Nowak, C.; Beer, B. C.; Pick, A.; Roth, T.; Lommes, P.; Sieber, V. A water-forming NADH oxidase from *Lactobacillus pentosus* suitable for the regeneration of synthetic biomimetic cofactors. *Frontiers in microbiology* **2015**, *6* (16), 957. DOI: 10.3389/fmicb.2015.00957.
- (2) Studier, F. W. Protein production by auto-induction in high-density shaking cultures. *Protein expression and purification* **2005**, *41* (1), 207–234.
- (3) Nowak, C.; Pick, A.; Lommes, P.; Sieber, V. Enzymatic reduction of nicotinamide biomimetic cofactors using an engineered glucose dehydrogenase: providing a regeneration system for artificial cofactors. *ACS Catal.* **2017**, *7* (8), 5202–5208. DOI: 10.1021/acscatal.7b00721.
- (4) Liu, H.; Naismith, J. H. An efficient one-step site-directed deletion, insertion, single and multiple-site plasmid mutagenesis protocol. *BMC Biotech.* **2008**, *8* (1), 1–10.
- (5) Eckert, K. A.; Kunkel, T. A. High fidelity DNA synthesis by the *Thermus aquaticus* DNA polymerase. *Nucleic Acids Res.* **1990**, *18* (13), 3739–3744.
- (6) Cline, J.; Braman, J. C.; Hogrefe, H. H. PCR fidelity of pfu DNA polymerase and other thermostable DNA polymerases. *Nucleic Acids Res.* **1996**, *24* (18), 3546–3551.
- (7) Fromant, M.; Blanquet, S.; Plateau, P. Direct random mutagenesis of gene-sized DNA fragments using polymerase chain reaction. *Anal. Biochem.* **1995**, *224* (1), 347–353.
- (8) Vanhercke, T.; Ampe, C.; Tirry, L.; Denolf, P. Reducing mutational bias in random protein libraries. *Anal. Biochem.* **2005**, *339* (1), 9–14.
- (9) Beckman, R. A.; Mildvan, A. S.; Loeb, L. A. On the fidelity of DNA replication: manganese mutagenesis in vitro. *Biochemistry* **1985**, *24* (21), 5810–5817.
- (10) Sperl, J. Etablierung von enzymatischer Aktivität auf künstlich erzeugten ($\beta\alpha$) 8-Barrel Proteinen, 2013.
- (11) Renzette, N. Generation of transformation competent *E. coli*. *Current Protocols in Microbiology* **2011**, *22* (1), A. 3L. 1-A. 3L. 5.